

Immunometabolic effects of lactate on humoral immunity in healthy individuals of different ages

Received: 25 August 2023

Accepted: 31 July 2024

Published online: 30 August 2024

 Check for updates

Maria Romero ^{1,3}, Kate Miller ^{1,3}, Andrew Gelsomini^{1,3}, Denisse Garcia ¹, Kevin Li ¹, Dhananjay Suresh ¹ & Daniela Frasca ^{1,2} 

Aging is characterized by chronic systemic inflammation and metabolic changes. We compare the metabolic status of B cells from young and elderly donors and found that aging is associated with higher oxygen consumption rates, and especially higher extracellular acidification rates, measures of oxidative phosphorylation and of anaerobic glycolysis, respectively. Importantly, this higher metabolic status, which reflects age-associated expansion of pro-inflammatory B cells, is found associated with higher secretion of lactate and autoimmune antibodies after in vitro stimulation. B cells from elderly individuals induce in vitro polarization of CD4⁺ T cells from young individuals into pro-inflammatory CD4⁺ T cells through metabolic pathways mediated by lactate, which can be inhibited by targeting lactate enzymes and transporters, as well as signaling pathways supporting anaerobic glycolysis. Lactate also induces immunosenescent B cells that are glycolytic, express transcripts for multiple pro-inflammatory molecules, and are characterized by a higher metabolic status. These results altogether may have relevant clinical implications and suggest alternative targets for therapeutic interventions in the elderly and patients with inflammatory conditions and diseases.

Lactate, the end product of anaerobic glycolysis, has been considered for long time a discarded metabolic compound, secreted under hypoxic conditions, with various harmful effects. However, increasing evidence indicates that lactate is an active metabolite in cell signaling and has a potent immunoregulatory role, especially at sites of inflammation where its accumulation is a common feature of inflammatory-based diseases including cancer^{1–4}. In healthy conditions, lactate is synthesized and consumed in almost every cell of the body, with the goal of keeping its blood concentration constant (1–3 mMol)⁵. However, in inflamed tissues [obese adipose tissue, tumor microenvironment, synovial tissue of rheumatoid arthritis (RA) patients, atherosclerotic plaques], as well as in the blood of patients with autoimmune diseases (Multiple Sclerosis, Sjogren's)^{6,7}, its concentration can rise significantly, reaching 10-fold higher levels. Lactate

effects are due to either signaling through its specific receptor, G protein-coupled receptor 81⁸, or to transport into cells through monocarboxylate transporters⁹.

Effects of lactate on immune cells have been described, with the majority of the findings showing pro-inflammatory rather than anti-inflammatory effects in dendritic cells^{10,11}, monocytes¹², macrophages^{13–15}, myeloid-derived suppressor cells (MDSCs)^{16,17}, CD8⁺ T cells¹⁸, CD4⁺ T cells³ and mast cells⁹. To our knowledge, effects on B cells have not been described yet. In this study, we have identified for the first time a key role for lactate in the regulation of B cell function and antibody production. We show that aging induces hypermetabolic B cells that are highly glycolytic and secrete large amounts of lactate. Lactate induces inflammatory B cells able to express multiple transcripts for markers of the senescence-associated

¹Department of Microbiology and Immunology, University of Miami Miller School of Medicine, Miami, FL, USA. ²Sylvester Comprehensive Cancer Center, University of Miami Miller School of Medicine, Miami, FL, USA. ³These authors contributed equally: Maria Romero, Kate Miller, Andrew Gelsomini.

 e-mail: dfrasca@med.miami.edu

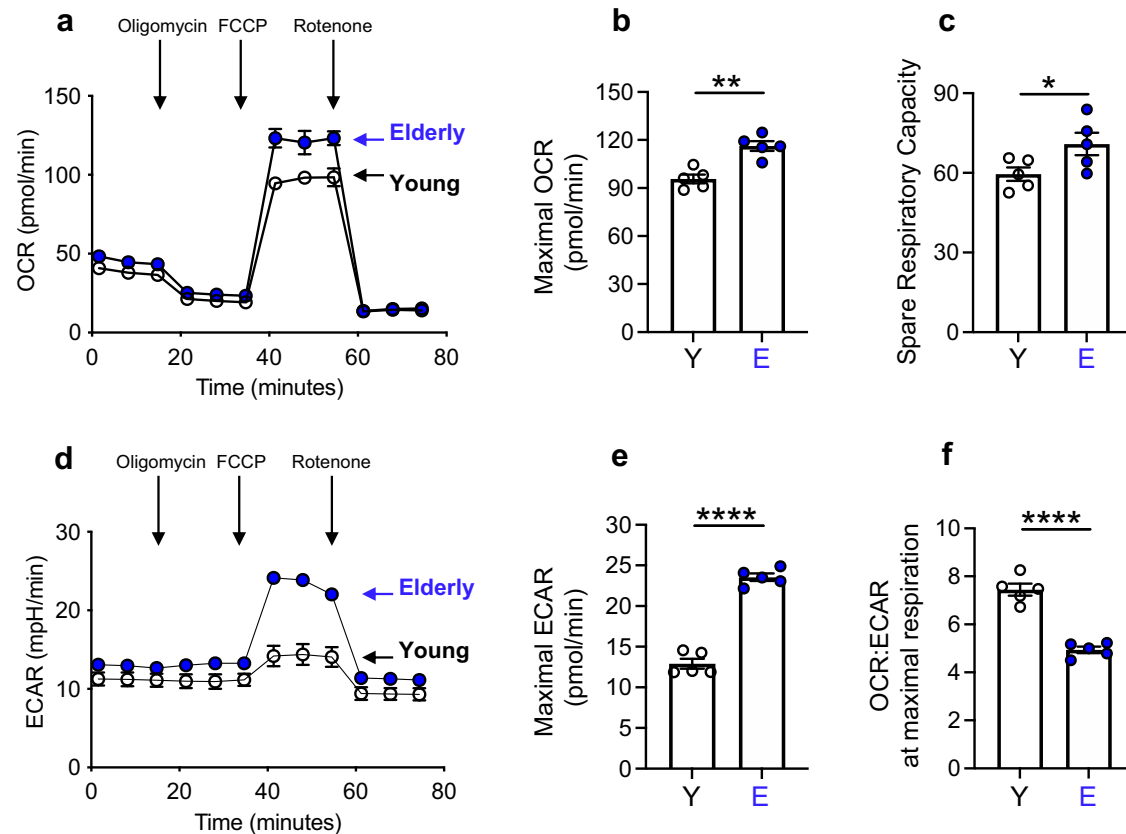


Fig. 1 | Aging induces hyper-metabolic B cells. B cells, isolated from the peripheral blood of young and elderly individuals using magnetic beads, were left unstimulated. B cells were seeded into the wells of an extracellular flux analyzer at the concentration of 2×10^5 /well in triplicate and run in a mitostress test. **a** OCR results representative of 5 independent experiments. **b** Maximal OCR. **c** Spare respiratory capacity (calculated subtracting basal OCR from maximal OCR values).

d ECAR results representative of five independent experiments. **e** Maximal ECAR. **f** OCR:ECAR at maximal respiration. Results show mean \pm Standard Error (SE) (with the exception of the experiments shown in **a** and **d**. Source data are provided as a Source Data file. Mean comparisons between groups were performed by unpaired Student's *t* test (two-tailed). **p* < 0.05, ***p* < 0.01, *****p* < 0.0001.

secretory phenotype (SASP) and to secrete autoimmune pathogenic antibodies. Moreover, we show that B cells from elderly individuals induce in vitro polarization of CD4⁺ T cells from young individuals into pro-inflammatory CD4⁺ T cells, and this occurs through metabolic pathways mediated by lactate secretion. Finally, we show that pharmacologic targeting of lactate enzymes and transporters, as well as of signaling pathways supporting anaerobic glycolysis, in B cells from elderly individuals inhibits their polarizing function, suggesting an alternative approach to target B cell-mediated inflammation. The effects of lactate described herein recapitulate key features of B cells that infiltrate inflammatory tissues, where lactate-induced signaling may promote many pathogenic features and persistence of the B cell infiltrates.

Results

Aging induces hyper-metabolic B cells

We evaluated the metabolic status of B cells isolated from the peripheral blood of young and elderly healthy individuals. Briefly, B cells were enriched from PBMC using CD19 magnetic beads. B cells were left unstimulated because we have previously shown that the status of unstimulated B cells is associated with their capacity to respond after in vivo or in vitro stimulation²⁰. We used Seahorse technology and the mitostress test that allow real-time evaluations of oxygen consumption rates (OCR), measures of oxidative phosphorylation (OXPHOS) and mitochondrial fitness, and extracellular acidification rates (ECAR), measures of anaerobic glycolysis and lactate secretion. In the mitostress test, the sequential addition of pharmacological drugs such as oligomycin (that blocks ATP synthase), FCCP (fluoro-carbonyl cyanide

phenylhydrazone, an uncoupling agent that allows maximal respiration) and Rotenone/Antimycin (that block maximal respiratory activity) alters the bioenergetic profile of the mitochondria. Results in Fig. 1 show higher OCR (a), higher maximal respiration (b) and higher spare respiratory capacity (c) in B cells from elderly versus young individuals. The differences in ECAR in B cells from elderly as compared to those from younger individuals are even bigger than those in OCR (d), with higher maximal ECAR (e) and lower ratio OCR:ECAR under maximal respiratory conditions (f). Collectively, these findings indicate that B cells from elderly individuals are able to switch more readily from OXPHOS to anaerobic glycolysis after ATP synthase is blocked by the addition of oligomycin in the mitostress test. No differences were observed in the other measures performed during the mitostress test (non mitochondrial respiration, coupling efficiency, proton leak, ATP production).

The composition of the circulating B cell pool changes with age as we and others have previously shown, with a significant expansion of the subsets of naive B cells and of Double Negative (DN) B cells, which is the most pro-inflammatory B cell subset, a decrease in the subset of switched memory B cells and no changes in IgM memory B cells^{21–23}. Therefore, we wanted to investigate the contribution of the B cell subsets that expand with age to the metabolic status of the B cell pool. The composition of the circulating B cell pool of the recruited young and elderly individuals is shown in Supplementary Fig. 1a–c. We sorted naive and DN B cell subsets and we measured OCR and ECAR using the mitostress test. Results show higher OCR and ECAR measures in both naive (Supplementary Fig. 2a–f) and DN (Supplementary Fig. 2g–l) B cell subsets from elderly individuals, with the higher values being

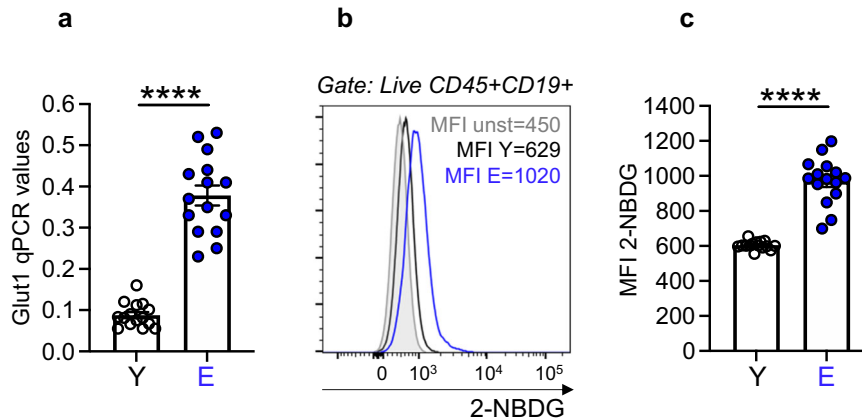


Fig. 2 | Aging induces higher glucose uptake in unstimulated B cells. B cells, isolated as in Fig. 1, were left unstimulated. **a** mRNA expression of the glucose transporter Glut1 measured by qPCR. Results show qPCR values ($2^{-\Delta C_t}$), mean \pm SE. **b** Representative flow cytometry histograms from one young and one elderly individual of glucose uptake measured by flow cytometry using the glucose

fluorescent analog 2-NBDG. Results show MFI (mean fluorescence intensity). **c** 2-NBDG MFI results from all individuals, mean \pm SE. Source data are provided as a Source Data file. Mean comparisons between groups were performed by unpaired Student's *t* test (two-tailed). **** $p < 0.0001$.

observed in DN versus naive B cells, clearly indicating that the metabolic status of the B cell pool of elderly individuals is mainly associated with the expansion of the DN B cell subset.

Aging induces glycolytic B cells

We wanted to confirm the above results by measuring by qPCR the expression of transcripts for enzymes involved in metabolic pathways associated with OCR and ECAR. In particular, we measured the expression of a member of the pyruvate dehydrogenase (PDH) complex, PDHX, that converts pyruvate into Acetyl CoA and therefore represents a link between glycolysis and Krebs's cycle, the production of reactive oxygen species, ROS, and the expression of lactate dehydrogenase A (LDHA), that converts pyruvate into lactate.

First, we measured by qPCR the expression of the transcript for glucose transporter 1 (Glut1), the major glucose transporter of human circulating B cells. Figure 2a shows higher expression of Glut1 RNA in unstimulated B cells from elderly individuals, as compared to those from younger controls. In a few young and elderly individuals, we compared RNA expression of the other Gluts (Glut1, Glut2, Glut3, Glut4). We found that human B cells also express higher levels of transcripts for Glut4, albeit at lower levels as compared to those for Glut1, and more in B cells from elderly versus young individuals. No age differences were found in transcripts for Glut2 and Glut3, both expressed at extremely low levels (Supplementary Fig. 3a–e). Sorted naive B cells show age differences in the expression of transcripts for Glut1 and Glut4 (Glut2 and Glut3 were undetectable, Supplementary Fig. 3f–i) but at significantly lower levels as compared to DN B cells (Supplementary Fig. 3j–m). We also measured glucose uptake by flow cytometry and the glucose fluorescent analog [2-(N-(7-Nitrobenz-2-oxa-1,3-diazol-4-yl)Amino)-2-Deoxyglucose], 2-NBDG. Figure 2b, c shows higher glucose uptake in unstimulated B cells from elderly versus young individuals, confirming the qPCR results on Glut1 expression. In both sorted naive and DN B cells, glucose uptake is lower in both B cell subsets from young individuals as compared to those from elderly individuals, with glucose uptake being higher in DN B cells versus naive B cells (Supplementary Fig. 3n–q). These results altogether demonstrate that DN B cells represent the cell type mainly if not exclusively responsible for the expression of transcripts for glucose transporters and for glucose uptake in the circulating B cell pool.

We then evaluated PDHX RNA expression and found it higher in unstimulated B cells from elderly versus young individuals (Fig. 3a), as well as the expression of cytosolic ROS, that reflects almost exclusively

mitochondrial ROS, as evaluated by flow cytometry and CellROX staining (Fig. 3b, c). Mitochondrial ROS was also measured in some individuals by flow cytometry and MitoSOX staining, with results showing similar age differences as those above (Fig. 3d). Moreover, B cells from young and elderly individuals show comparable total mitochondrial mass, as evaluated by flow cytometry and the mitochondrial probe MitoTracker Green (Fig. 3e, f), but increased mRNA expression of the peroxisome proliferator-activated receptor- γ coactivator 1 α (PPARGC1 α) (Fig. 3g), a co-transcriptional regulator involved in mitochondrial biogenesis²⁴. When we evaluated mitochondrial markers in sorted naive and DN B cell subsets, PDHX expression and cytosolic ROS (Supplementary Fig. 4a–f), as well as mitochondrial mass and PPARGC1 α (Supplementary Fig. 4g–l), were found lower in both subsets from young versus elderly individuals, with values higher in DN B cells versus naive B cells.

Although PDHX RNA expression and ROS production were significantly higher in unstimulated B cells from elderly as compared to those from younger individuals, the biggest difference was observed in RNA expression of LDHA (Fig. 4a) and lactate secretion (Fig. 4b). LDHA transcripts were evaluated in unstimulated B cells whereas lactate secretion was quantified by ELISA after B cell stimulation for 48 hrs with the mitogen CpG. Autoimmune antibody secretion was evaluated in the same CpG-stimulated B cell cultures after 7 days (Fig. 4c). We demonstrated that secretion of double strand (ds)DNA-specific IgG autoimmune antibodies is induced by lactate which promotes RNA expression of *tbx21*, T-bet, the transcription factor for autoimmune antibodies^{25–27} (Fig. 4d). Antibodies were positively and significantly associated with lactate (Fig. 4e). Dose-response experiments showed that 10 mM was the optimal dose to induce in vitro secretion of autoimmune antibodies (Supplementary Fig. 5a). Other autoimmune specificities were also measured (Supplementary Fig. 5b–e). These results are to our knowledge the first to show that lactate induces autoimmune pathogenic B cells and is a stimulus for autoimmune antibody secretion. When we evaluated markers of anaerobic glycolysis in sorted naive and DN B cell subsets, we found LDHA expression, lactate and autoimmune antibody secretion lower in both subsets from young versus elderly individuals. Again, values were higher in DN B cells versus naive B cells (Supplementary Fig. 6a–f), with autoimmune antibodies and lactate being positively and significantly associated only in DN B cells (Supplementary Fig. 6g, h). Not only LDHA, but also other enzymes in anaerobic glycolysis pathways, were found expressed at higher levels in DN B cells from elderly versus young individuals (Supplementary Fig. 6i).

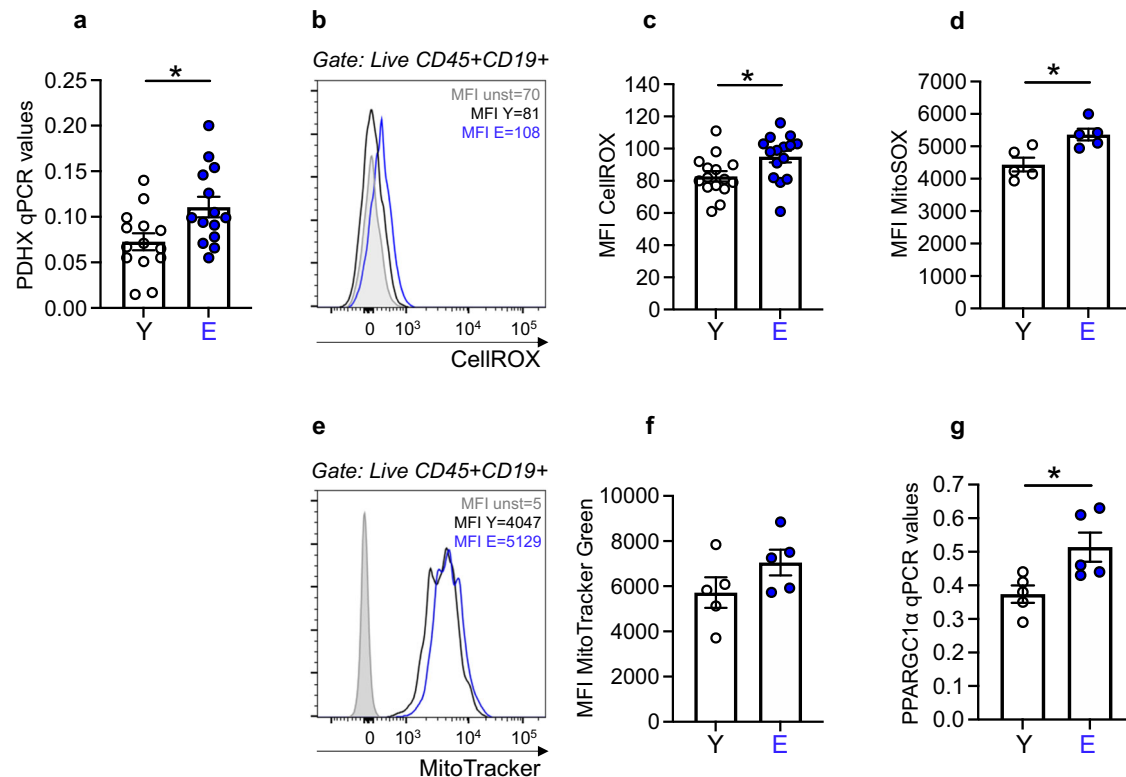


Fig. 3 | Aging increases mitochondrial function in unstimulated B cells. B cells, isolated as in Fig. 1, were left unstimulated. **a** mRNA expression of PDHX. Results show qPCR values ($2^{-\Delta C_t}$), mean \pm SE. **b** Representative flow cytometry histograms from one young and one elderly individual of cytoplasmic ROS staining using the fluorescent compound CellROX. **c** Cytoplasmic ROS MFI results from all individuals, mean \pm SE. **d** Mitochondrial ROS MFI results from all individuals after staining with the fluorescent compound MitoSOX, mean \pm SE. **e** Representative flow

cytometry histograms from one young and one elderly individual of mitochondrial mass staining using the MitoTracker Green probe. **f** MitoTracker Green MFI results from all individuals, mean \pm SE. **g** mRNA expression of PPARGC1 α . Results show qPCR values ($2^{-\Delta C_t}$), mean \pm SE. Source data are provided as a Source Data file. Mean comparisons between groups were performed by unpaired Student's t test (two-tailed). * $p < 0.05$.

Metabolic measures in the 4 sorted B cells subsets from young and elderly individuals are shown in Supplementary Table 1. Seahorse OCR and ECAR results on maximal respiration are shown in Supplementary Table 2 for the subset of swlg memory B cells only, as the number of IgM memory B cells, as we have shown in Supplementary Fig. 1, is too low to perform the mitostress test.

B cells from elderly individuals induce pro-inflammatory CD4+ T cells through metabolic pathways

We then evaluated if hyper-metabolic B cells from elderly individuals were also capable to polarize CD4+ T cells from young individuals making them hyper-metabolic, inflammatory and pathogenic. To do so, we set up co-cultures in which CD4+ T cells from young individuals were positioned in the top part of a transwell, whereas B cells from young or elderly individuals were positioned at the bottom of the transwell (Supplementary Fig. 7a). After 24 hrs, CD4+ T cells were harvested and evaluated by qPCR for the expression of transcripts for Glut1, LDHA and PDHX, whereas after 48 hrs, supernatants were tested for the presence of the T cell-derived pro-inflammatory cytokines IL-17A and IFN- γ . Figure 5a shows that CD4+ T cells from young individuals were able to up-regulate the expression of transcripts for Glut1 and LDHA, and to a lesser extent for PDHX, only in the presence of B cells from elderly individuals, whereas no effect was observed if B cells were from young individuals. Figure 5b shows that supernatants from co-cultures of young CD4+ T cells with B cells from elderly but not young individuals were enriched in the T cell-derived pro-inflammatory cytokines IL-17A and IFN- γ at 48 hrs. In these supernatants other pro-inflammatory cytokines (IL-6 and TNF- α), as well as IL-10, were also

enriched but to a lesser extent (Supplementary Fig. 7b–d), whereas no changes were observed for IL-2 and IL-4 (Supplementary Fig. 7e, f). To confirm the above findings showing that B cells from young individuals were not able to polarize CD4+ T cells towards a pro-inflammatory phenotype, in a few experiments we co-cultured B cells from young individuals with CD4+ T cells from both young and elderly individuals. Results show that secretion of IL-17A and IFN- γ in elderly CD4+ T cells co-cultured with young B cells were comparable to that of elderly CD4+ T cells cultured alone without any B cells. Moreover, secretion in elderly CD4+ T cells co-cultured with elderly B cells (or with elderly DN B cells) was found to be higher than that in young CD4+ T cells co-cultured with elderly B cells (Supplementary Table 3).

CD4+ T cells from young individuals, co-cultured with B cells from elderly individuals, showed higher OCR and ECAR profiles when tested in a mitostress test as compared to those co-cultured with B cell from young individuals (Fig. 5c, d). Co-culture supernatants were also tested for the presence of lactate (Fig. 5e). We found lactate only in co-cultures set up in the presence of B cells from elderly individuals. In these conditions, lactate comes exclusively from B cells, as CD4+ T cells need to be heavily stimulated with the mitogens PMA and Ionomycin to secrete lactate. Moreover, the amount of lactate in these co-cultures is much less than that measured in CpG-stimulated B cells (see Fig. 4b). CD4+ T cells from young individuals co-cultured with B cells from elderly individuals show NF- κ B activation, measured by the translocation from the cytoplasm to the nucleus of RelA/p65, as compared to those that are co-cultured with B cells from young individuals (Fig. 5f), suggesting that the lactate induction of pro-inflammatory cytokine secretion occurs through NF- κ B, as also

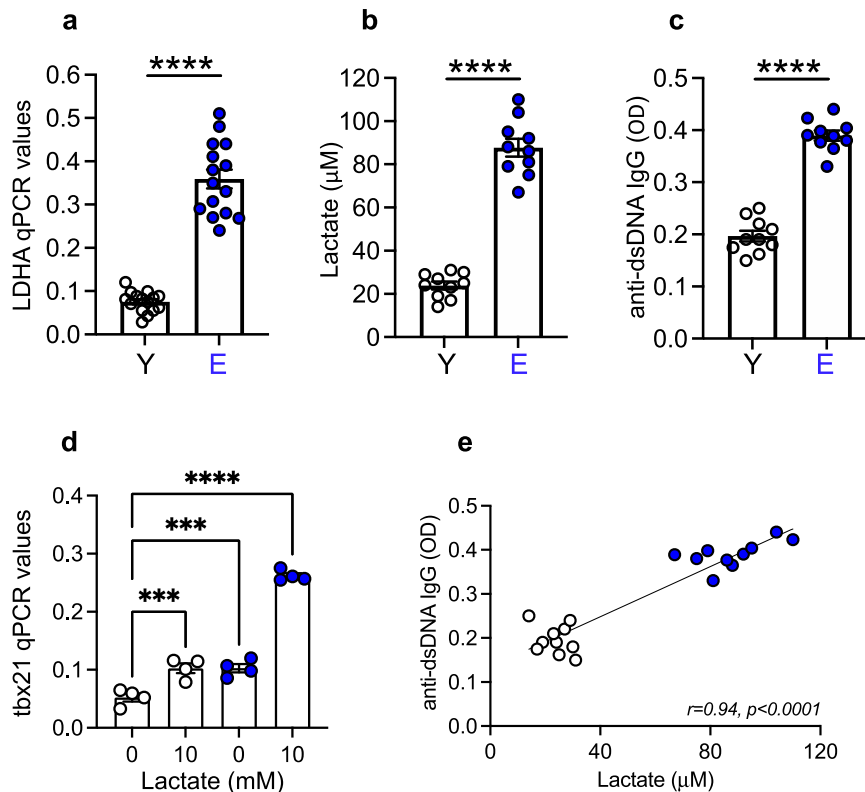


Fig. 4 | Aging increases anaerobic glycolysis in unstimulated B cells. B cells, isolated as in Fig. 1, were left unstimulated. **a** mRNA expression of LDHA. Results show qPCR values ($2^{-\Delta Ct}$), mean \pm SE. **b** Lactate secretion in culture supernatants of CpG-stimulated B cells (48 hrs) measured by ELISA, mean \pm SE. **c** Anti-dsDNA autoimmune IgG antibodies in culture supernatants of CpG-stimulated B cells (7 days) measured by ELISA, mean \pm SE. **d** mRNA expression of *tbx21* in CpG-

stimulated B cells (24 hrs) in the absence or presence of lactate (10 mM). Results show qPCR values ($2^{-\Delta Ct}$), mean \pm SE. **e** Correlation of lactate and autoimmune IgG. Pearson's r and p values are shown at the bottom of the figure. Source data are provided as a Source Data file. Mean comparisons between groups were performed by unpaired Student's t test (two-tailed). *** $p < 0.001$, **** $p < 0.0001$.

previously shown in our mouse experiments²⁸. In the same co-cultures, we also measured by flow cytometry levels of phosphorylated STAT3 (signal transducer and activator of transcription 3, p-STAT3), a constitutive activator of NF- κ B²⁹ (Fig. 5g). Results show increased p-STAT3 levels in CD4+ T cells co-cultured with B cells as compared with those cultured alone, with p-STAT3 significantly higher in CD4+ T cells co-cultured with B cells from elderly versus young individuals. Moreover, the polarizing function of B cells from elderly individuals in these co-cultures, is due to the subset of DN B cells, as naive B cells from elderly individuals show no polarizing effect and all pro-inflammatory cytokines were undetected (Supplementary Fig. 7g, h).

We next tried to block lactate using specific inhibitors as shown in Supplementary Fig. 7i, j and evaluate if blocking lactate was reducing IL-17A and IFN- γ secretion. We used three different lactate inhibitors: FX11, [3-dihydroxy-6-methyl-7-(phenylmethyl)-4-propyl-naphthalene-1-carboxylic acid], a small molecule that blocks the enzyme LDHA; anti-SLC5A12, a polyclonal antibody that inhibits the lactate transporter SLC5A12 acting as an electroneutral and low affinity sodium-dependent solute transporter that catalyzes the transport across the membrane of many monocarboxylates including lactate; anti-ICOSL, an antibody that inhibits the interaction between B cells expressing the ligand for the inducible T cell costimulatory molecule (ICOSL) and CD4+ T cells expressing ICOS. This interaction has been shown to induce glucose uptake and activation of anaerobic glycolysis, leading to the generation of pro-inflammatory T cells³⁰. Figure 6a shows that pre-inclusion of B cells from elderly individuals with FX11 before the co-culture significantly inhibits the secretion of IL-17A. However, when we used the anti-SLC5A12 antibody (Fig. 6b) or the anti-ICOSL antibody (Fig. 6c), the inhibition was even more effective (Fig. 6b, c). Similar

results were obtained for IFN- γ secretion (Fig. 6d-f). All treatments were able to significantly decrease lactate secretion by B cells from elderly individuals in these co-cultures, with a better effect of anti-SLC5A12 anti-ICOSL as compared to FX11 (Fig. 6g-i). IL-6, TNF- α and IL-10 were also decreased in the co-cultures set-up in the presence of B cells from elderly individuals pre-treated with FX11, anti-SLC5A12 and anti-ICOSL, with more inhibition being observed when B cells were pre-treated with anti-SLC5A12 and anti-ICOSL as compared to FX11, whereas no effects of lactate inhibitors were observed for IL-2 and IL-4 secretion, as shown in Source Data file.

Lactate induces immunosenescent B cells that are hyper-glycolytic and hyper-inflammatory

Next, we wanted to examine if lactate was also able to induce pro-inflammatory B cells, similar to what we have described above for CD4+ T cells. Briefly, B cells from young individuals were stimulated overnight with GpG in the presence or absence of lactate. Then, cultures were harvested and cells loaded on a glycolytic test in Seahorse performed with sequential addition of glucose, oligomycin and 2-DG. Figure 7a shows that lactate induces a hyper-glycolytic phenotype in B cells from young individuals which is confirmed by expression of *Glut1* and *LDHA* transcripts and, to a lesser extent, of *PDHX* (Fig. 7b). B cells stimulated overnight in the presence of lactate look indistinguishable from B cells from elderly individuals, clearly indicating that lactate induces immunosenescence in B cells from young individuals. Lactate increases expression of transcripts for multiple inflammatory markers, many of which are members of the SASP, Fig. 7c. These include pro-inflammatory cytokines and chemokines (TNF, IL-6, IL-8), pro-inflammatory microRNAs (miRs) involved in class switch and antibody

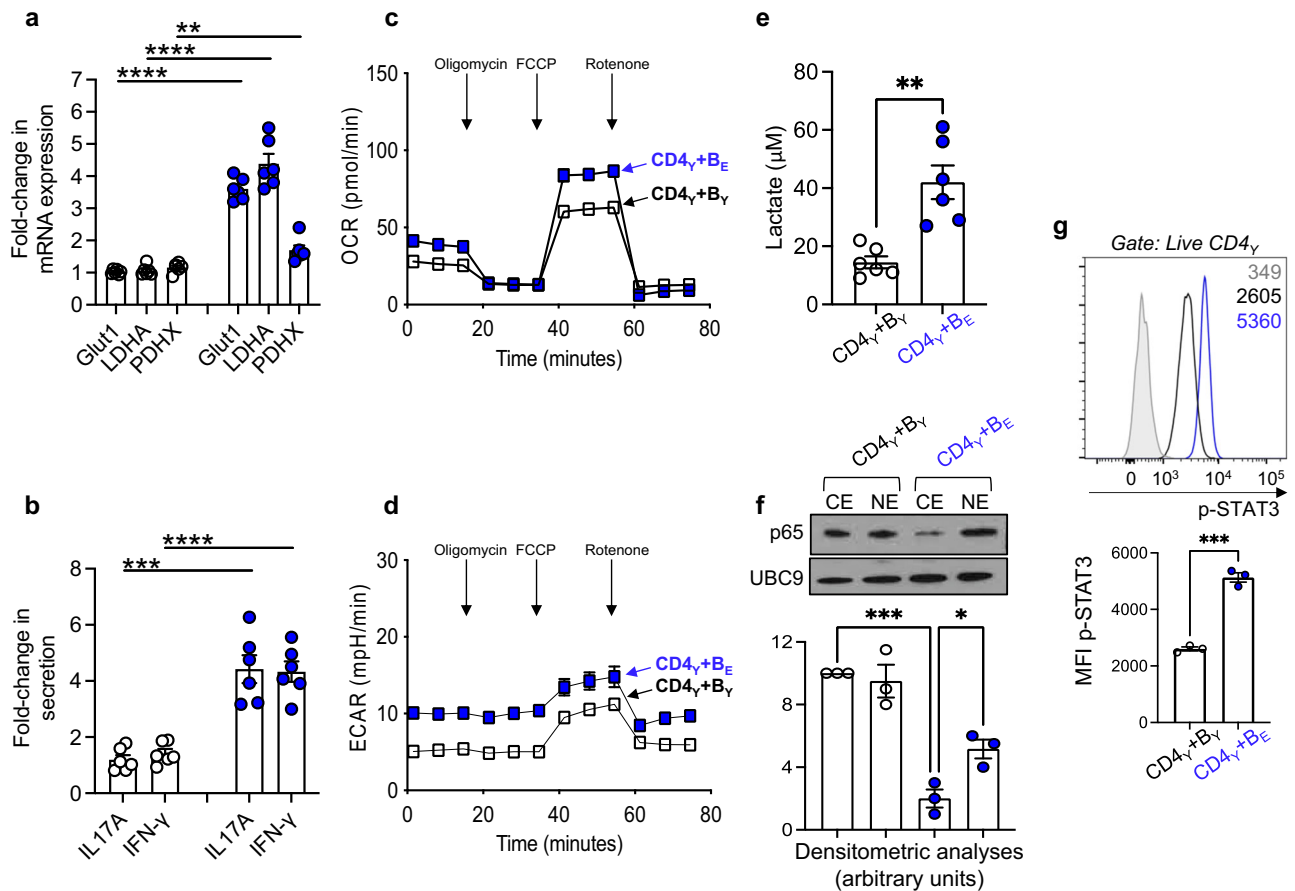


Fig. 5 | B cells from elderly individuals induce pro-inflammatory CD4 $^+$ T cells through metabolic and inflammatory pathways. B cells from young (white symbols) and elderly (blue symbols) individuals were cultured at the bottom of transwells together with CD4 $^+$ T cells, sorted from young individuals, placed at the top of transwells. After 24 hrs, CD4 $^+$ T cells were harvested, mRNA extracted and qPCR performed. **a** Fold-change in RNA expression of metabolic markers (Glut1/LDHA/PDHX). Fold-change is the ratio of RNA expression in CD4 $^+$ T cells co-cultured with B cells (from either young or elderly individuals)/RNA expression in CD4 $^+$ T cells co-cultured without B cells. Results show mean \pm SE. **b** Fold-change in cytokine secretion (IL-17A/IFN- γ) measured by CBA. Fold-change is the ratio of IL-17A and IFN- γ in co-cultures with B cells (from either young or elderly individuals)/IL-17A and IFN- γ in co-cultures without B cells (only CD4 $^+$ T cells). Results show mean \pm SE. **c, d** CD4 $^+$ T cells from co-cultures with B cells from young or elderly individuals were run at the concentration of 2×10^5 /well in triplicate in a mitostress

test. OCR and ECAR results are representative of two independent experiments. **e** Lactate measured in co-cultures of B cells from young or elderly individuals after 48 hrs by ELISA, mean \pm SE. **f** Cytoplasmic (CE) and nuclear (NE) protein extracts (5 μ g/lane) from CD4 $^+$ T cells from young individuals, co-cultured with B cells from young or elderly individuals, were blotted with the indicated antibodies. Results are representative of 3 independent experiments. Densitometric analyses of p65 normalized to UBC9 are shown for these samples below the images, mean \pm SE. **g** Top, representative flow cytometry histograms of p-STAT3 in CD4 $^+$ T cells after co-culture with B cells from either young (black) or elderly (blue) individuals, as compared to CD4 $^+$ T cells alone (gray), same individuals in **f**. Bottom, MFI results from all 3 individuals, mean \pm SE (MFI from CD4 $^+$ T cells alone = 349 ± 33). Source data are provided as a Source Data file. Mean comparisons between groups were performed by unpaired Student's t test (two-tailed). **p < 0.01, ***p < 0.001, ****p < 0.0001.

secretion (miR-155, miR-16), markers of immune activation (TLR2, TLR4) and cell cycle inhibitors (p16^{INK4a}, p21^{CIP1/WAF1}). In line with the expression of SASP transcripts, B cells from young individuals CpG-stimulated overnight with lactate were positively stained with the marker of immunosenescence β -Galactosidase, similar to B cells from elderly individuals (Fig. 7d). After 48 hrs of CpG stimulation in the presence of lactate, B cells from young individuals, similar to those from elderly individuals, secrete IL-6 and TNF- α in culture supernatants (Fig. 7e, f), and after 7 days also secrete autoimmune pathogenic antibodies (Fig. 7g).

The effects of lactate on B cells from elderly individuals occur because B cells express the lactate transporter SLC5A12, as shown in Supplementary Fig. 8a. The expression is low but detectable on CpG-stimulated B cells from young individuals and is upregulated by the overnight stimulation in the presence of lactate. In this condition, SLC5A12 expression is comparable to what is observed in CpG-stimulated B cells from elderly individuals. SLC5A12 expression can be effectively inhibited after a short incubation of B cells with the

neutralizing antibody specific for the transporter, and higher is the expression of SLC5A12 higher is the level of inhibition (Supplementary Fig. 8b). In the presence of the anti-SLC5A12 neutralizing antibody, secretion of IL-6 and TNF- α as well of autoimmune pathogenic antibodies is inhibited in B cells from young individuals incubated in the presence of lactate (Fig. 8a–c), and in B cells from elderly individuals (Fig. 8d–f).

Discussion

Results in this paper show that B cells from elderly individuals are hyper-metabolic and hyper-inflammatory, as compared to those from younger controls, with a higher OCR and especially a higher ECAR status, clearly indicating that they can effectively switch from OXPHOS to anaerobic glycolysis after ATP synthase is blocked in the mitostress test. Due to their hyper-glycolytic status, B cells from elderly individuals synthesize lactate after in vitro stimulation with the mitogen CpG and secrete pathogenic autoimmune antibodies. Lactate secreted by B cells from elderly individuals is at least one of the crucial players in the

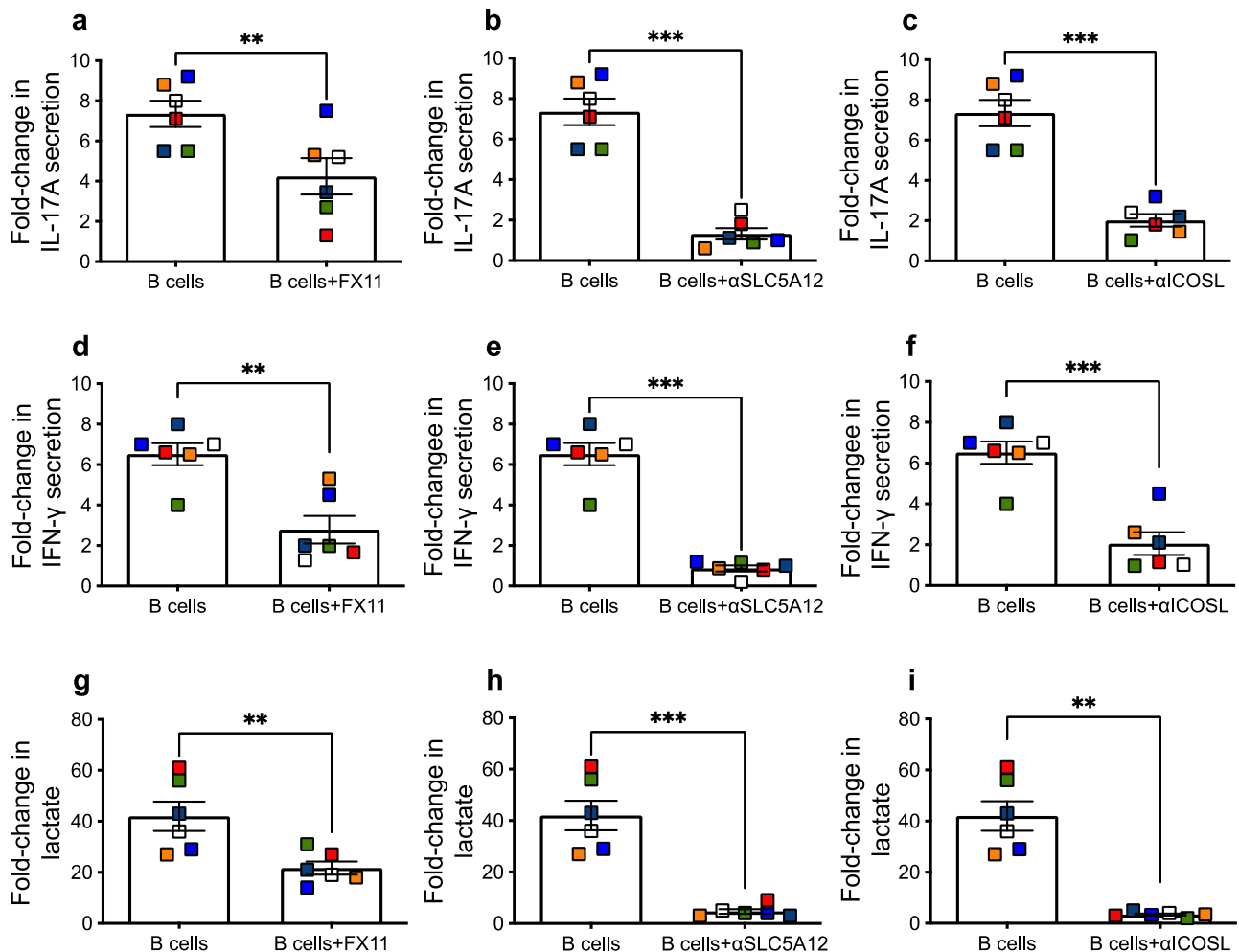


Fig. 6 | Lactate inhibition decreases the polarizing effect of B cells from elderly individuals. B cells from elderly individuals were cultured at the bottom of transwells together with CD4⁺ T cells from young individuals, placed at the top of transwells. B cells were left untreated or pre-treated overnight with FX11 (10 mM/10⁶ B cells), or with anti-SLC5A12 (1:500 dilution), or with anti-ICOSL (10 μg/mL), before CD4⁺ T cells were added at the top of the transwell. Supernatants were collected after 48 hrs to measure IL-17A and IFN-γ secretion by CBA. Results show

fold-change in IL-17A secretion (a–c), or in IFN-γ secretion (d–f), calculated as the ratio of IL-17A or IFN-γ in co-cultures with B cells from elderly individuals, either untreated or treated/IL-17A, IFN-γ in co-cultures without B cells (only CD4⁺ T cells). Results are mean ± SE. g–i Lactate measured in co-cultures of B cells untreated or treated with FX11, anti-SLC5A12 or anti-ICOSL, mean ± SE. Source data are provided as a Source Data file. Mean comparisons between groups were performed by paired Student's t test (two-tailed). ***p* < 0.01, ****p* < 0.001.

polarization of CD4⁺ T cells from young individuals into pro-inflammatory CD4⁺ T cells, in agreement with the observation that inhibition of lactate enzymes and transporters decreases the pro-inflammatory phenotype of CD4⁺ T cells by decreasing IL-17A and IFN-γ secretion. These lactate-induced polarizing effects confirm previously published observations showing that sustained enzymatic activity of LDHA is necessary for the secretion of pro-inflammatory cytokines by CD4⁺ T cells, and inhibition of LDHA significantly decreases glucose uptake and promotes a shift to OXPHOS while reducing pro-inflammatory cytokine secretion³¹.

These polarizing effects of B cells from elderly but not from young individuals are particularly significant in inflamed tissues where lactate accumulates (obese adipose tissue, inflamed RA joints, tumor microenvironment). Lactate in fact induces up-regulation of the SLC5A12 transporter, which in turn induces lactate uptake, activating a local series of events and a positive loop of inflammation. Here we show the expression of the SLC5A12 transporter on B cells from young individuals and to a higher level of expression on B cells from elderly individuals. The expression of the transporter is higher in B cells as compared to CD4⁺ T cells³. Targeting the SLC5A12 transporter has already shown promising results

in a pre-clinical model of RA in which SLC5A12 expression correlates with disease activity³. Not only lactate enzymes and transporters, but also signaling pathways that support anaerobic glycolysis, can be targeted to improve local inflammatory conditions. It has indeed been shown that inflamed synovial joints of RA patients are enriched in ICOS⁺ T cells interacting with ICOSL⁺ B cells³⁰, with ICOS-ICOSL signaling being able to enhance glucose uptake and anaerobic glycolysis, leading to the generation of pro-inflammatory T cells. Blocking ICOSL on B cells dramatically reduces the expression of chemokine receptors involved in the B cell-driven recruitment of T cells to inflamed tissues, whereas blocking ICOS signal on T cells successfully inhibits the expression of glycolytic enzymes and the secretion of pro-inflammatory cytokines such as IL-17A and IFN-γ³⁰. Our findings herein, together with this aforementioned study, suggest that B cell-specific therapies, such as anti-CD20 antibodies in patients with autoimmune diseases may successfully be used not only to reduce tissue damage due to the secretion of pathogenic autoimmune antibodies, but also to block their polarizing capacity.

Our results herein also address for the first time the effects of lactate on the generation of immunosenescent, inflammatory,

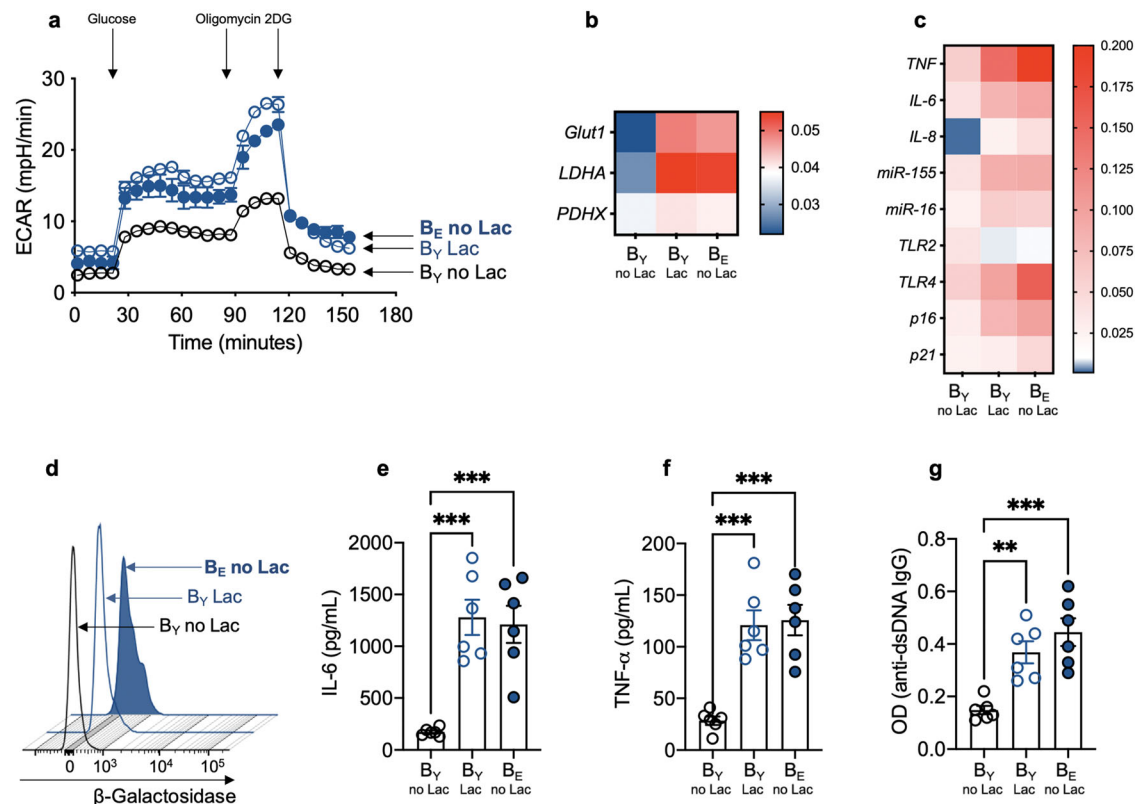


Fig. 7 | Lactate induces immunosenescent B cells that are hyper-glycolytic and hyper-inflammatory. B cells from young (B_Y) and elderly (B_E) individuals, isolated as in Fig. 1, were stimulated overnight with CpG ($5 \mu\text{g}/10^6$ cells). B cells from young individuals were also stimulated with CpG+lactate ($10 \text{ mM}/10^6$ B cells). **a** Cells were seeded into the wells of an extracellular flux analyzer at the concentration of 2×10^5 /well and run in a glycolytic test. **b** Expression of transcripts for metabolic markers. **c** Expression of transcripts for pro-inflammatory markers. Heatmaps in **b**, **c** show qPCR values ($2^{-\Delta\text{CT}}$) of multiple pro-inflammatory markers, normalized to

GAPDH. **d** Staining with β -Galactosidase. Results show MFI from one representative experiment (values from all individuals, mean \pm SE, are: 130 ± 5 , young; 243 ± 29 , young+lactate; 296 ± 35 , elderly no lactate). **e** IL-6 in culture supernatants after 48 hrs measured by CBA, mean \pm SE. **f** TNF- α in culture supernatants after 48 hrs measured by CBA, mean \pm SE. **g** Autoimmune IgG antibodies after 7 days measured by ELISA, mean \pm SE. Source data are provided as a Source Data file. Mean comparisons were performed by two-way ANOVA. *** $p < 0.001$.

pathogenic B cells. It is already known that anaerobic glycolysis and lactate secretion, together with the enzyme LDHA, are upregulated in many types of non immune and immunosenescent cells. These pathways are needed for the secretion of markers of the SASP³², cell and endoplasmic reticulum enlargement, that occur concomitantly with NF- κ B signaling and activation. The induction of immunosenescent B cells by lactate, which is present at high concentration in inflamed tissues, such as the joints of RA patients^{33,33}, the tumor microenvironment^{34,35}, the obese adipose tissue^{36–38}, has a significant pathological role as immunosenescent B cells not only secrete inflammatory mediators and pathogenic antibodies, but they can also induce senescence in other immune cell types that infiltrate the inflamed tissue through the SASP. Therefore, targeting lactate may significantly reduce not only the pathogenicity of B cells, but also lactate effects on other immune (T cells, macrophages, monocytes, dendritic cells, MDSCs) and non immune cell types (endothelial cells, synoviocytes, tumor cells), leading to decreased secretion of inflammatory mediators and amelioration of local inflammatory conditions.

In conclusion, our results show that the pathogenic function of B cells in elderly individuals is metabolically supported. These findings are particularly relevant for conditions and diseases in which B cells interact in a cell-to-cell way with other cell types, as in inflamed tissues, turning them into pro-inflammatory cells that contribute to local inflammatory pathways and pathogenicity. Our findings offer a rationale for the development of therapies that selectively target B cell metabolic products involved in the generation of inflammatory, immunosenescent, pathogenic immune cells.

Methods

Subjects

Participants were young (30–45 years) and elderly (≥ 65 years), all recruited at the University of Miami Miller School of Medicine. Participants were healthy and were not taking medications affecting the immune system. Subjects with type-2 diabetes mellitus, autoimmune diseases, congestive heart failure, cardiovascular disease, chronic renal failure, malignancies, renal or hepatic diseases, infectious disease, trauma or surgery, pregnancy, or under substance and/or alcohol abuse were excluded.

All participants signed an informed consent. The study was reviewed and approved by our Institutional Review Board (IRB, protocols #20070481 and #20160542), which reviews all human research conducted under the auspices of the University of Miami. Characteristics of the recruited participants (age, gender, serum metabolic measures) are shown in Supplementary Table 4. Briefly, young participants are 30–45 year-old, whereas elderly participants are ≥ 65 year-old. Participants are 50% males and 50% females. In every experiment, same numbers of male and female participants have been evaluated.

PBMC collection

Blood was drawn in Vacutainer CPT tubes (BD 362761), then PBMC were isolated and cryopreserved. PBMC were thawed and cultured at the concentration of 1×10^6 /mL in complete medium (c-RPMI) [RPMI 1640 (Gibco ThermoFisher 11875-093), supplemented with 10% FBS (Gibco 10437-028), 100 U/mL Penicillin-Streptomycin (Gibco 15140-122), and 2 mM L-glutamine Gibco 25030-081)]. FBS was certified to be

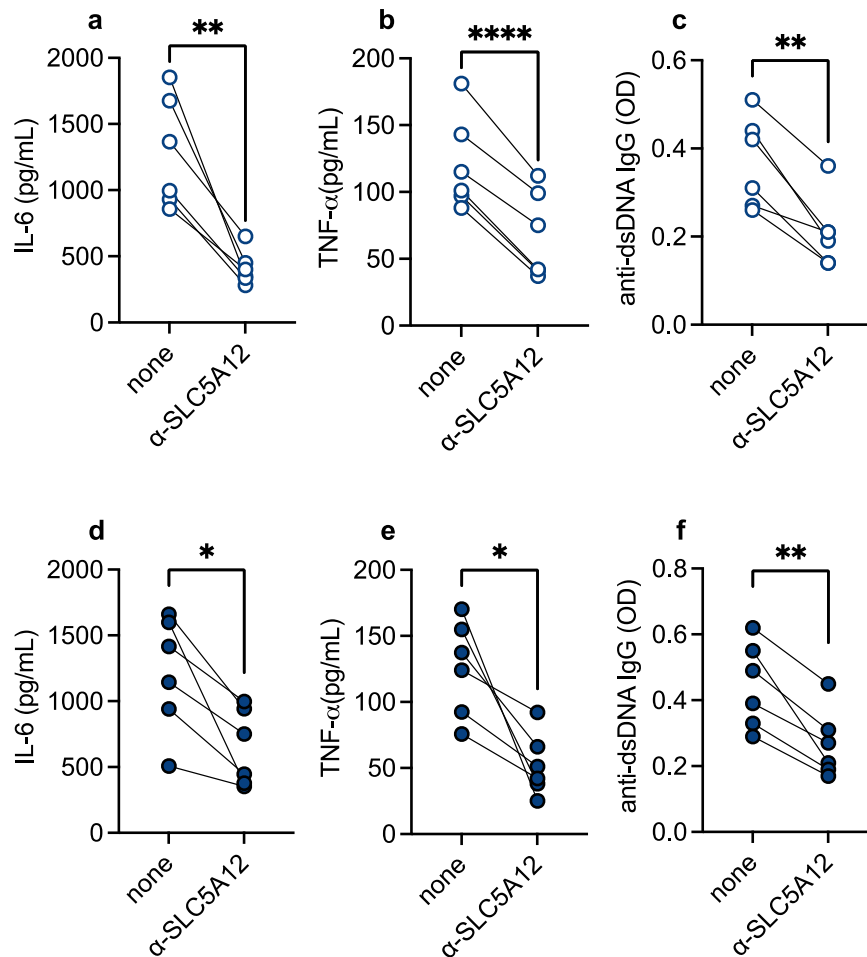


Fig. 8 | The effects of lactate on B cells from young individuals, as well as on those from elderly individuals, are decreased by inhibition of the lactate transporter. B cells from young and elderly individuals, isolated as in Fig. 1, were stimulated overnight with CpG ($5 \mu\text{g}/10^6$ cells). B cells from young individuals were stimulated with CpG in the presence of lactate ($10 \text{ mM}/10^6$ cells) and secretion of IL-

6, TNF- α and autoimmune IgG was measured in cultures of B cells from young individuals+lactate (a–c) or in those from elderly (d–f) individuals. Results show mean \pm SE. Source data are provided as a Source Data file. Mean comparisons between groups were performed by paired Student's t test (two-tailed). * $p < 0.05$, ** $p < 0.001$, **** $p < 0.0001$.

endotoxin-free. After thawing, viability of the PBMC was checked by trypan blue counting and samples were discarded if viability was $<75\%$.

B cell isolation and in vitro stimulation

B cells were isolated from thawed PBMC by magnetic sorting using CD19 Microbeads (Miltenyi Biotec 130-121-301) according to the MiniMACS protocol ($20 \mu\text{L}$ Microbeads + $80 \mu\text{L}$ PBS, for 10^7 cells). Cell preparations were typically $>95\%$ pure, as evaluated by flow cytometry.

B cells at the concentration of $10^6/\text{mL}$ of c-RPMI were left unstimulated or were stimulated 2–7 days with $5 \mu\text{g}/10^6$ cells of CpG (ODN 2006 Invivogen). In glycolytic experiments, B cells were stimulated overnight with CpG ($5 \mu\text{g}/10^6$ cells), in the absence or presence of lactate (Na-Lactate, SIGMA 98867-56-1, $10 \text{ mM}/10^6$ cells). In dose-response experiments, lactate was used at concentrations of 1–20 mM/ 10^6 B cells.

To evaluate RNA expression of molecules involved in metabolic pathways, the mRNA was extracted from unstimulated or stimulated B cells with μMACS mRNA isolation kit (Miltenyi Biotec), eluted into $75 \mu\text{L}$ of pre-heated (65°C) elution buffer, and stored at -80°C until use.

To evaluate the expression of inflammatory markers, unstimulated or stimulated B cells were resuspended in TRIzol (Ambion) (10^6 cells/ $100 \mu\text{L}$), then RNA extracted for qPCR. Total RNA was isolated according to the manufacturer's protocol, eluted into $10 \mu\text{L}$ of pre-heated elution buffer and stored at -80°C until use.

Culture supernatants were collected at day 2 of CpG stimulation to measure the secretion of pro- and anti-inflammatory cytokines by BD™ Cytometric Bead Array, CBA (BD 560484) human TH1/TH2/TH17 kit, or lactate using the L-lactate assay kit (Cayman Chemicals 700510), following manufacturer's instructions. Day-7 supernatants were evaluated for autoimmune IgG antibodies by ELISA (MyBioSource MBS390120).

B cell:CD4+ T cell co-cultures

B cells, sorted from young or elderly individuals, were cultured at the bottom of transwells (Costar 3396) together with CD4+ T cells, sorted from young individuals, placed at the top of transwells. CD4+ T cells were also cultured in transwell without B cells. The ratio B:CD4+ T cells was reflecting the ratio of these cell types in ex vivo isolated PBMC. After 24 hrs, CD4+ T cells were harvested, mRNA extracted and qPCR performed. Supernatants were also collected after 48 hrs for cytokine and lactate secretion measured by CBA and ELISA, respectively.

In some co-cultures, B cells were left untreated or were pre-treated overnight with the small molecule FX11 [3-dihydroxy-6-methyl-7-(phenylmethyl)-4-propyl-naphthalene-1-carboxylic acid] that inhibits the enzyme LDHA (EMD Millipore 427218), or with a polyclonal antibody blocking the lactate transporter SLC5A12 (ThermoFisher Invitrogen PA5-110389), or with an anti-ICOSL antibody (ThermoFisher Invitrogen 16-5889-82), before CD4+ T cells were added to the top of

the transwell. Lactate inhibitors were used as follows: 10 mM/10⁶ B cells (FX11), 1:500 dilution (anti-SLC5A12), 10 µg/10⁶ B cells (anti-ICOSL).

Flow cytometry

PBMC (2 × 10⁶/mL) were membrane stained for 20 min at room temperature with Live/Dead kit and with the following antibodies: anti-CD45 (Biolegend 368540), anti-CD19 (BD 555415), anti-CD27 (BD 555441) and anti-IgD (BD 555778) to measure naive (IgD+CD27-), IgM memory (IgD+CD27+), switched memory (IgD-CD27+), and DN (IgD-CD27-) B cells.

For the evaluation of glucose uptake, cytosolic ROS, mitochondrial ROS and mitochondrial mass, PBMC were initially stained with the metabolic reagents and then with Live/Dead kit and the antibodies above (anti-CD45/CD19/CD27/IgD). For glucose uptake we used the fluorescent glucose analog (2-(N-(7-Nitrobenz-2-oxa-1,3-diazol-4-yl) Amino)-2-Deoxyglucose) (2-NBDG, Thermo Fisher N13195). For cytosolic ROS we used CellROX[®] Deep Red Reagent (Thermo Fisher C10422), whereas for mitochondrial ROS we used with MitoSOX[™] Red (mitochondrial superoxide indicators, Thermo Fisher M36009). For mitochondrial mass we used MitoTracker Green (Thermo Fisher M7514). Working concentrations were recommended by the manufacturers. Staining was at room temperature for 30 minutes. Cells were then washed twice with FACS buffer, and then membrane stained for 20 minutes at room temperature. For phosphorylated STAT3 (p-STAT3), CD4+ T cells were membrane stained initially with Live/Dead kit and anti-CD4 (Biolegend 317410), then fixed, permeabilized with PBS-0.2% Tween, then stained for additional 20 min at room temperature with anti-phospho-STAT3 antibody (Tyr 705, Cell Signaling 4113S), followed by an anti-IgG (H + L) secondary conjugated antibody (Thermo Fisher A11029). For β-Galactosidase staining, we used the Cellular Senescence detection kit SPiDER β-Gal (Dojindo Molecular Technologies SG04) at concentrations recommended by the manufacturer, but after membrane staining. In every experiment we acquired up to 10⁵ events in the B cell gate on a LSR-Fortessa (BD). Results were analyzed using FlowJo 10.5.3 software. Single color controls were included in every experiment for compensation. Isotype controls were also used in every experiment to set up the gates.

Sorting of the B cell subsets

B cell subsets were sorted in a Sony SH800 cell sorter using anti-CD45, anti-CD19, anti-CD27 and anti-IgD antibodies. Cell preparations were typically >98% pure. naive and DN B cells were stimulated with CpG (5 µg/10⁶ cells) in the presence of an AffiniPure F(ab')₂ fragment of goat anti-human IgG+IgM (anti-Ig) (2 µg/10⁶ cells; Jackson ImmunoResearch Laboratories 109-006-127), the anti-Ig antibody being necessary for optimal stimulation of naive B cells.

Reverse Transcriptase (RT) and quantitative (q)PCR

RT reactions were performed in a Mastercycler Eppendorf Thermo-cycler to obtain cDNA. Briefly, 10 µL of mRNA from freshly isolated cells, or 2 µL of total RNA (from Trizol, Ambion) at the concentration of 0.5 µg/µL, were used as template for cDNA synthesis in the RT reaction. For miR quantification, RNA was reverse transcribed in the presence of specific primers (provided together with the qPCR primers).

Five µL of cDNA were used for qPCR. Reactions were conducted in MicroAmp 96-well plates and run in the ABI 7500 machine. Calculations were made with ABI software. For calculations, we determined the cycle number at which transcripts reached a significant threshold (Ct) for target genes and GAPDH (control). The difference in Ct values between GAPDH and the target gene was calculated as ΔCt. Then the relative amount of the target gene was expressed as 2^{-ΔCt} and indicated as qPCR values. All reagents were from Thermo Fisher. Taqman primers were: GAPDH, Hs99999905_m1; Glut1/SLC2A1, Hs00892681; Glut2/SLC2A2, Hs01096908_m1; Glut3/SLC2A3, Hs00359840_m1; Glut4/SLC2A4, Hs00168966_m1; Hexokinase 1, HK1, Hs00175976_m1; Hexokinase 2,

HK2, Hs006086_m1; 6-phosphofructo-2-kinase/fructose-2,6-biphosphatase 1, PFKFB1, HS00997227_m1; Enolase 1, ENO1, Hs00361415_m1; Enolase 2, ENO2, Hs00157360_m1; Pyruvate kinase M1/2, PKM, Hs00761782_s1; LDHA, Hs01378790_g1; LDHB, Hs00929956_m1; PDHX, Hs00185790_m1; PPARGC1α, Hs00173304_m1; SLC5A12, Hs01054645; tbx21, Hs00894392_m1; TNF, Hs01113624_g1; IL-6, Hs00985639_m1; IL-8, Hs00174103_m1; TLR2, Hs02621280_s1; TLR4, Hs00152939_m1; p16^{INK4} (CDKN2A), Hs00923894_m1; p21^{CIP1/WAF1}, Hs00355782_m1; U6, 001973; miR-155, 002623; miR-16, 000391.

Preparation of cytoplasmic and nuclear protein extracts and Western blot

Proteins were extracted from CD4+ T cells from young individuals after 48 hrs co-culture without or with B cells from elderly individuals. Cytoplasmic and nuclear protein extracts were prepared from the same numbers of cells. Briefly, cells were centrifuged in a 5415 C Eppendorf microfuge (322 g, 5 min.). The pellet was resuspended in 20 µL of solution A containing Hepes 10 mM, pH 7.9, KCl 10 mM, EDTA 1.0 mM, DTT 1 mM, MgCl₂ 1.5 mM, PMSF 1 mM, 1 tablet of protease inhibitor cocktail (Boeringer Mannheim, Germany) (per 20 mL, 1 mM Na₃VO₄ and Nonidet P-40 (0.1%), briefly vortexed and centrifuged (5152 × g, 5 min, 4 °C). The supernatant containing the cytoplasmic extract (CE) was removed and stored at -80 °C. To obtain nuclear extracts (NE), the pellet containing the nuclei was resuspended in solution B containing Hepes 20 mM, pH 7.9, EDTA 0.1 mM, DTT 1 mM, MgCl₂ 1.5 mM, PMSF 2 mM, 1 tablet of protease inhibitor cocktail (per 20 mL), and glycerol 10%. The lysate was incubated on ice for 20 min, protein sonicated for a few seconds and centrifuged (15,777 × g, 15 min, 4 °C). Aliquots of NE were stored at -80 °C. Protein contents were determined by Bradford assay³⁹. The amount of protein extracted from the same number of B cells from both young and elderly individuals is highly reproducible (90%) from one experiment to another.

CE and NE were electrophoresed in denaturing conditions and then electro-transferred on nitrocellulose filters. Filters were incubated with the following primary antibodies in PBS-Tween 20 containing 5% milk: mouse monoclonal UBC9 (1:1000 diluted, BD Bioscience 610748), mouse monoclonal NF-κB p65 (1:200 diluted, Santa Cruz Biotechnology sc-8008). After overnight incubation with the primary antibodies, immunoblots were incubated with the secondary antibody goat anti-mouse IgG (1:50,000 diluted, Jackson ImmunoResearch Labs 115-035-003) for 3 hrs at room temperature. Membranes were developed by enzyme chemiluminescence and exposed to CL-XPosure Film (Pierce). Films were scanned and analyzed using the Alphascreen Enhanced Resolution Gel Documentation & Analysis System (Alpha Innotech, San Leandro CA) and images were quantitated using the AlphaEaseFC 32-bit software. Full scan blots are shown in Source Data file.

Mitostress test

The metabolic profile of unstimulated B cells from young and elderly individuals was evaluated by the mitostress test and Seahorse technology that allows real-time evaluation of changes in oxygen consumption rates (OCR) and extracellular acidification rates (ECAR), measures of oxidative phosphorylation and of anaerobic glycolysis, respectively. In some experiments, the metabolic profile of unstimulated CD4+ T cells from young individuals, harvested after co-culture with B cells from either young or elderly individuals, was also investigated. The mitostress test was conducted in a Seahorse XFp extracellular flux analyzer (Agilent). Briefly, B cells, at the concentration of 2.5 × 10⁵/well, were initially incubated in Seahorse XF DMEM Medium (Agilent 103575) supplemented with 2 mM glutamine (Agilent 103579), 10 mM glucose (Agilent 103577) and 1 mM pyruvate (Agilent 103578), (200 µL of each reagent in 20 mL of medium). Maximal respiratory capacity was measured by treating with Oligomycin (1 µM) to block ATP production, followed by the uncoupling agent FCCP (fluoro-

carbonyl cyanide phenylhydrazone, 5 μ M), to dissipate proton gradients and allow electron transport and oxygen consumption to operate at maximal rate. This elevated OCR is suppressed by Rotenone/Antimycin (1 μ M), showing that respiration is mitochondrial.

Glycolytic test

First, B cells were incubated in Seahorse XF DMEM Medium without glucose. The first injection is a saturating concentration of glucose (10 mM). The second injection is oligomycin, at a concentration of 3.5 μ M. Oligomycin inhibits mitochondrial ATP production, and shifts the energy production to glycolysis, with the subsequent increase in ECAR revealing the cellular maximum glycolytic capacity. The final injection is 2-deoxy-glucose (2-DG, 20 mM), a glucose analog, that inhibits glycolysis through competitive binding to glucose hexokinase, the first enzyme in the glycolytic pathway. The resulting decrease in ECAR confirms that the ECAR produced in the experiment is due to glycolysis.

Statistical analyses

To examine differences between 3 groups, two-way ANOVA was used. Group-wise differences were analyzed afterwards with Bonferroni's multiple comparisons test, with $p < 0.05$ set as criterion for significance. To examine differences between 2 groups, paired Student's *t* test (two-tailed) was used. To examine relationships between variables, bivariate Pearson's correlation analyses were performed. GraphPad Prism version 10 software was used to construct all graphs.

Reporting summary

Further information on research design is available in the Nature Portfolio Reporting Summary linked to this article.

Data availability

The data and materials supporting this publications are available at <https://www.immport.org/shared/study/SDY2711>, <https://doi.org/10.21430/M3RA0B6YOY>. Source data are provided with this paper.

References

- Haas, R. et al. Intermediates of metabolism: from bystanders to signalling molecules. *Trends Biochem. Sci.* **41**, 460–471 (2016).
- Haas, R. et al. Lactate regulates metabolic and pro-inflammatory circuits in control of T cell migration and effector functions. *PLoS Biol.* **13**, e1002202 (2015).
- Pucino, V. et al. Lactate buildup at the site of chronic inflammation promotes disease by inducing CD4(+) T cell metabolic rewiring. *Cell Metab.* **30**, 1055–1074 e1058 (2019).
- Weyand, C. M., Zeisbrich, M. & Goronzy, J. J. Metabolic signatures of T-cells and macrophages in rheumatoid arthritis. *Curr. Opin. Immunol.* **46**, 112–120 (2017).
- Nichol, A. D. et al. Relative hyperlactatemia and hospital mortality in critically ill patients: a retrospective multi-centre study. *Crit. Care* **14**, R25 (2010).
- Amorini, A. M. et al. Serum lactate as a novel potential biomarker in multiple sclerosis. *Biochim. Biophys. Acta* **1842**, 1137–1143 (2014).
- Pucino, V., Bombardieri, M., Pitzalis, C. & Mauro, C. Lactate at the crossroads of metabolism, inflammation, and autoimmunity. *Eur. J. Immunol.* **47**, 14–21 (2017).
- Lee, Y. J. et al. G-protein-coupled receptor 81 promotes a malignant phenotype in breast cancer through angiogenic factor secretion. *Oncotarget* **7**, 70898–70911 (2016).
- Srinivas, S. R. et al. Cloning and functional identification of slc5a12 as a sodium-coupled low-affinity transporter for monocarboxylates (SMCT2). *Biochem. J.* **392**, 655–664 (2005).
- Caronni, N. et al. Downregulation of membrane trafficking proteins and lactate conditioning determine loss of dendritic cell function in lung cancer. *Cancer Res.* **78**, 1685–1699 (2018).
- Gottfried, E. et al. Tumor-derived lactic acid modulates dendritic cell activation and antigen expression. *Blood* **107**, 2013–2021 (2006).
- Dietl, K. et al. Lactic acid and acidification inhibit TNF secretion and glycolysis of human monocytes. *J. Immunol.* **184**, 1200–1209 (2010).
- Samuvel, D. J., Sundararaj, K. P., Nareika, A., Lopes-Virella, M. F. & Huang, Y. Lactate boosts TLR4 signaling and NF-kappaB pathway-mediated gene transcription in macrophages via monocarboxylate transporters and MD-2 up-regulation. *J. Immunol.* **182**, 2476–2484 (2009).
- Shime, H. et al. Tumor-secreted lactic acid promotes IL-23/IL-17 proinflammatory pathway. *J. Immunol.* **180**, 7175–7183 (2008).
- Zhou, H. C. et al. Lactic acid in macrophage polarization: the significant role in inflammation and cancer. *Int. Rev. Immunol.* **41**, 4–18 (2022).
- Husain, Z., Seth, P. & Sukhatme, V. P. Tumor-derived lactate and myeloid-derived suppressor cells: Linking metabolism to cancer immunology. *Oncoimmunology* **2**, e26383 (2013).
- Yang, X. et al. Lactate-modulated immunosuppression of myeloid-derived suppressor cells contributes to the radioresistance of pancreatic cancer. *Cancer Immunol. Res.* **8**, 1440–1451 (2020).
- Fischer, K. et al. Inhibitory effect of tumor cell-derived lactic acid on human T cells. *Blood* **109**, 3812–3819 (2007).
- Caslin, H. L. et al. Lactic acid inhibits lipopolysaccharide-induced mast cell function by limiting glycolysis and ATP Availability. *J. Immunol.* **203**, 453–464 (2019).
- Frasca, D., Diaz, A., Romero, M., Landin, A. M. & Blomberg, B. B. High TNF-alpha levels in resting B cells negatively correlate with their response. *Exp. Gerontol.* **54**, 116–122 (2014).
- Frasca, D., Diaz, A., Romero, M., D'Eramo, F. & Blomberg, B. B. Aging effects on T-bet expression in human B cell subsets. *Cell Immunol.* **321**, 68–73 (2017).
- Frasca, D., Diaz, A., Romero, M., Thaller, S. & Blomberg, B. B. Metabolic requirements of human pro-inflammatory B cells in aging and obesity. *PLoS One* **14**, e0219545 (2019).
- Frasca, D. et al. Obesity decreases B cell responses in young and elderly individuals. *Obesity* **24**, 615–625 (2016).
- Callender, L. A. et al. GATA3 induces mitochondrial biogenesis in primary human CD4(+) T cells during DNA damage. *Nat. Commun.* **12**, 3379 (2021).
- Naradikian, M. S. et al. Cutting edge: IL-4, IL-21, and IFN-gamma interact to govern T-bet and CD11c expression in TLR-activated B cells. *J. Immunol.* **197**, 1023–1028 (2016).
- Peng, S. L., Szabo, S. J. & Glimcher, L. H. T-bet regulates IgG class switching and pathogenic autoantibody production. *Proc. Natl. Acad. Sci. USA* **99**, 5545–5550 (2002).
- Rubtsova, K., Rubtsov, A. V., van Dyk, L. F., Kappler, J. W. & Marrack, P. T-box transcription factor T-bet, a key player in a unique type of B-cell activation essential for effective viral clearance. *Proc. Natl. Acad. Sci. USA* **110**, E3216–E3224 (2013).
- Li, K. et al. B cells from old mice induce the generation of inflammatory T cells through metabolic pathways. *Mech. Ageing Dev.* **209**, 111742 (2023).
- Surh, Y. J., Bode, A. M. & Dong, Z. Breaking the NF-kappaB and STAT3 alliance inhibits inflammation and pancreatic tumorigenesis. *Cancer Prev. Res.* **3**, 1379–1381 (2010).
- Zeng Q. H. et al. B cells polarize pathogenic inflammatory T helper subsets through ICOSL-dependent glycolysis. *Sci Adv* **6**, eabb6296 (2020).
- Peng, M. et al. Aerobic glycolysis promotes T helper 1 cell differentiation through an epigenetic mechanism. *Science* **354**, 481–484 (2016).
- Wiley, C. D. et al. Mitochondrial dysfunction induces senescence with a distinct secretory phenotype. *Cell Metab.* **23**, 303–314 (2016).

33. Yi, O. et al. Lactate metabolism in rheumatoid arthritis: pathogenic mechanisms and therapeutic intervention with natural compounds. *Phytomedicine* **100**, 154048 (2022).
34. Bonuccelli, G. et al. Ketones and lactate “fuel” tumor growth and metastasis: evidence that epithelial cancer cells use oxidative mitochondrial metabolism. *Cell Cycle* **9**, 3506–3514 (2010).
35. de la Cruz-Lopez, K. G., Castro-Munoz, L. J., Reyes-Hernandez, D. O., Garcia-Carranca, A. & Manzo-Merino, J. Lactate in the regulation of tumor microenvironment and therapeutic approaches. *Front. Oncol.* **9**, 1143 (2019).
36. Ahmed, K. et al. An autocrine lactate loop mediates insulin-dependent inhibition of lipolysis through GPR81. *Cell Metab.* **11**, 311–319 (2010).
37. DiGirolamo, M., Newby, F. D. & Lovejoy, J. Lactate production in adipose tissue: a regulated function with extra-adipose implications. *FASEB J.* **6**, 2405–2412 (1992).
38. Lin, Y. et al. Lactate is a key mediator that links obesity to insulin resistance via modulating cytokine production from adipose tissue. *Diabetes* **71**, 637–652 (2022).
39. Bradford, M. M. A rapid and sensitive method for the quantitation of microgram quantities of protein utilizing the principle of protein-dye binding. *Anal. Biochem.* **72**, 248–254 (1976).

Acknowledgements

This study is supported by NIH award AG32576 (D.F.) and by CFAR Emerging Opportunity-FY2022-xx award (D.F.). The authors would like to thank the volunteers who participated in this study, and the personnel of the Department of Family Medicine and Community Health at the University of Miami Miller School of Medicine, in particular Dr. Robert Schwartz, Chairman, for the recruitment of study participants. The authors also thank Dr. Bonnie Blomberg for sharing lab space and reagents.

Author contributions

D.F. wrote the paper and was involved in funding acquisition. D.F., M.R., K.M., A.G., D.G., K.L., and D.S. performed the experiments and analyzed data. All authors have seen and approved the manuscript.

Competing interests

The authors declare no competing interests.

Additional information

Supplementary information The online version contains supplementary material available at <https://doi.org/10.1038/s41467-024-51207-x>.

Correspondence and requests for materials should be addressed to Daniela Frasca.

Peer review information *Nature Communications* thanks Jenna Bartley and the other, anonymous, reviewers for their contribution to the peer review of this work. A peer review file is available.

Reprints and permissions information is available at <http://www.nature.com/reprints>

Publisher’s note Springer Nature remains neutral with regard to jurisdictional claims in published maps and institutional affiliations.

Open Access This article is licensed under a Creative Commons Attribution-NonCommercial-NoDerivatives 4.0 International License, which permits any non-commercial use, sharing, distribution and reproduction in any medium or format, as long as you give appropriate credit to the original author(s) and the source, provide a link to the Creative Commons licence, and indicate if you modified the licensed material. You do not have permission under this licence to share adapted material derived from this article or parts of it. The images or other third party material in this article are included in the article’s Creative Commons licence, unless indicated otherwise in a credit line to the material. If material is not included in the article’s Creative Commons licence and your intended use is not permitted by statutory regulation or exceeds the permitted use, you will need to obtain permission directly from the copyright holder. To view a copy of this licence, visit <http://creativecommons.org/licenses/by-nc-nd/4.0/>.

© The Author(s) 2024